We are IntechOpen,
the world's leading publisher of
Open Access books
Built by scientists, for scientists

4,800
Open access books available

122,000
International authors and editors

135M
Downloads

Our authors are among the

154
Countries delivered to

TOP 1%
most cited scientists

12.2%
Contributors from top 500 universities

CLARIVATE ANALYTICS
BOOK CITATION INDEX
INDEXED

WEB OF SCIENCE™

Selection of our books indexed in the Book Citation Index
in Web of Science™ Core Collection (BKCI)

Interested in publishing with us?
Contact book.department@intechopen.com

Numbers displayed above are based on latest data collected.
For more information visit www.intechopen.com

Power System Modelling for Urban Massive Transportation Systems

Mario A. Ríos and Gustavo Ramos
Universidad de los Andes, Bogotá, D.C.,
Colombia

1. Introduction

Urban Massive Transportation Systems (UMTS), like metro, tramway, light train; requires the supply of electric power with high standards of reliability. So, an important step in the development of these transportation systems is the electric power supply system planning and design.

Normally, the trains of a UMTS requires a DC power supply by means of rectifier AC/DC substations, know as traction substations (TS); that are connected to the electric HV/MV distribution system of a city. The DC system feeds catenaries of tramways or the third rail of metros, for example. The DC voltage is selected according to the system taking into account power demand and length of the railway's lines. Typically, a 600 Vdc – 750 Vdc is used in tramways; while 1500 Vdc is used in a metro system. Some interurban-urban systems use a 3000 Vdc supply to the trains.

Fig. 1 presents an electric scheme of a typical traction substation (TS) with its main components: AC breakers at MV, MV/LV transformers, AC/DC rectifiers, DC breakers, traction DC breakers. As, it is shown, a redundant supply system is placed at each traction substation in order to improve reliability. In addition, some electric schemes allow the power supply of the catenaries connected to a specific traction substation (A) since the neighbour traction substation (B) by closing the traction sectioning between A and B and opening the traction DC breakers. In this way, the reliability supply is improved and allows flexibility for maintenance of TS.

So, an important aspect for the planning and design of this electric power supply is a good estimation of power demand required by the traction system that will determine the required number, size and capacity of AC/DC rectifier substations. On the other hand, the design of the system requires studying impacts of the traction system on the performance of the distribution system and vice versa. Power quality disturbances are present in the operation of these systems that could affect the performance of the traction system.

This chapter presents useful tools for modelling, analysis and system design of Electric Massive Railway Transportation Systems (EMRTS) and power supply from Distribution Companies (DisCo) or Electric Power Utilities. Firstly, a section depicting the modelling and simulation of the power demand is developed. Then, a section about the computation of

the placement and sizing of TS for urban railway systems is presented where the modelling is based on the power demand model of the previous section. After that, two sections about the power quality (PQ) impact of EMRTS on distribution systems and grounding design are presented. Both subjects make use of the load demand model presented previously.
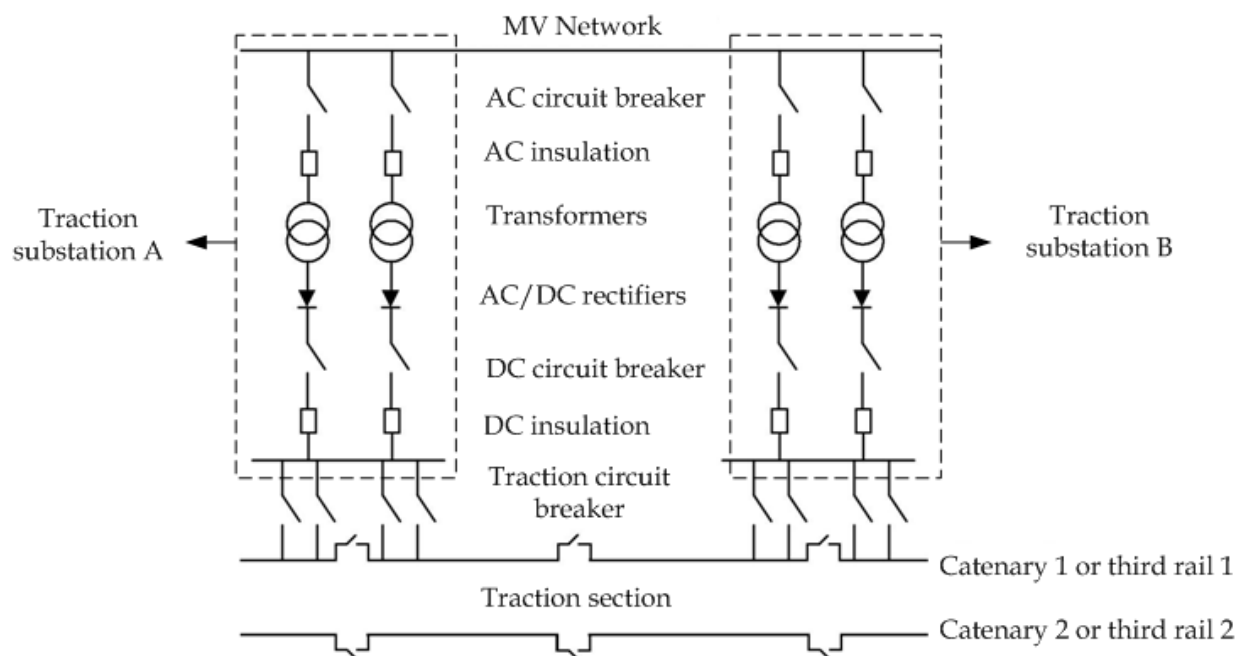

Fig. 1. A Typical Traction Substation (TS)

2. Power demand computation of electric transportation systems

This section presents a mathematical model useful to simulate urban railway systems and to compute the instantaneous power of the Electric Massive Railway Transportation Systems (EMRTS) such as a metro, light train or tramway, by means of computing models that take into account parameters such as the grid size, acceleration, velocity variation, EMRTS braking, number of wagons, number of passengers per wagon, number of rectifier substations, and passenger stations, among other factors, which permit to simulate the physical and electric characteristics of these systems in a more accurate way of a real system.

This model connects the physical and dynamic variables of the traction behaviour with electrical characteristics to determine the power consumption. The parametric construction of the traction and braking effort curves is based on the traction theory already implemented in locomotives and urban rails. Generally, there are three factors that limit the traction effort versus velocity: the maximum traction effort (F_{max}) conditioned by the number of passengers that are in the wagons, the maximum velocity of the train (or rail), and the maximum power consumption. Based on these factors, a simulation model is formulated for computing the acceleration, speed and placement of each train in the railway line for each time step (1 second, for example). So, the power consumption or re-generation is computed also for each time step and knowing the placement of each train in the line, the power demand for each electric TS is calculated.

2.1 Power consumption model of an urban train

The power consumed by one railway vehicle depends on the velocity and acceleration that it has at each instant of time. Its computation is based on the traction effort characteristic (supplied by the manufacturer of the motors), the number of passengers and the distances between the passengers' stations (Vukan, 2007), (Chen et al., 1999), (Perrin & Vernard, 1991). The duty cycle of an urban train between two passengers' stations is composed by four operation states: acceleration, balancing speed, constant speed and deceleration. Fig. 2 shows the behavior of the speed, traction effort and power consumption of a traction vehicle during each operation state elapsed either time or space (Hsiang & Chen, 2001).
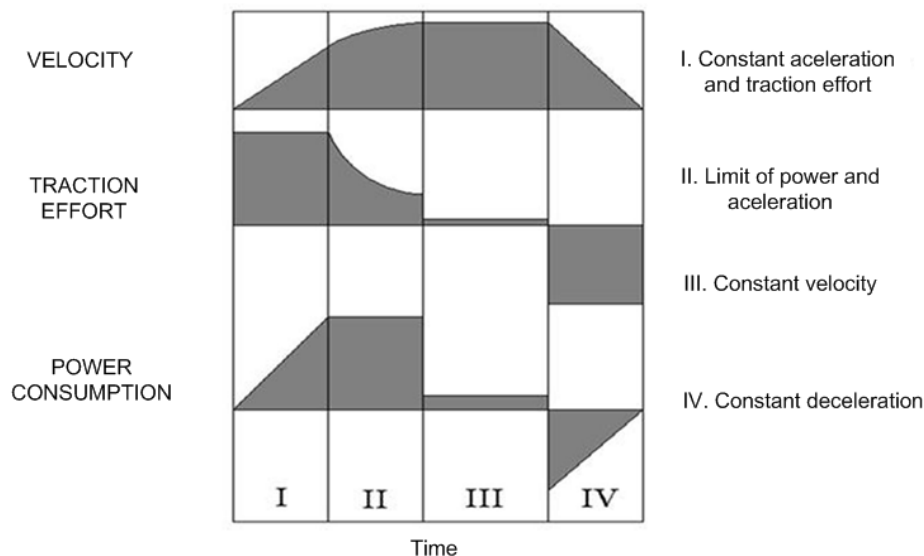

Fig. 2. Velocity, Traction Effort, and Power Consumption of an Urban Train Travel between adjacent Passenger Stations (Hsiang & Chen, 2001)

During the first state (I), the vehicle moves with constant positive acceleration, so the speed increases. When the vehicle reaches a determined speed lower than the constant speed, the second operation state starts. In this state, the acceleration decreases, but the speed keeps increasing. In the third state (III), the cruise speed is reached and the acceleration is zero. In the fourth state (IV), the braking operation starts with negative acceleration until the moment it decelerates with a constant rate and finally it stops at the destination station (Vukan, 2007), (Chen et al., 1999), (Perrin & Vernard, 1991), (Hsiang & Chen, 2001).

2.1.1 Net force of a traction vehicle

The parametric construction of the traction and braking effort curves is based on the traction theory already implemented in locomotives and high speed rails. Three factors limit the traction effort versus velocity: the maximum traction effort F_{max} conditioned by the number of passengers that are in the wagon, the maximum velocity of the vehicle, and the maximum power consumption. The maximum traction effort used by the acceleration, and then transferred to the rail, is limited by the total weight of the axles given by:

$$m_m = TM - (n_{axis} - n) \times w_{axle} \qquad (1)$$

where TM is the total vehicle mass, n is the number of motor drives, n_{axis} the number of axles in the vehicle, and w_{axle} the weight per axle (Buhrkall, 2006). The total vehicle mass is:

$$TM = w_v + \left(n_p \times w_{pas}\right) \times M_{DYN} \qquad (2)$$

where w_v corresponds to the weight per wagon without passengers, n_p the number of passengers per wagon, w_{pas} the average weight per passenger, and M_{DYN} the dynamic mass of the railway, which represents the stored energy in the spinning parts of the vehicle, typically of 5-10% (Buhrkall, 2006). Then, the maximum traction effort is calculated as:

$$F_{max} = \mu \times m_m \times g \qquad (3)$$

Where μ corresponds to the friction coefficient between the wheels and the rail, which is about 15% for the ERMTS, and gravity g equals to 9.8 m/s^2 (Buhrkall, 2006). The force needed to move a traction vehicle (TM times the acceleration (a)) is:

$$F = TM \times a = TM\frac{dv}{dt} = TE(v) - MR(v) - B_e(v) \qquad (4)$$

Where $TE(v)$ is the traction effort in an EMRTS that provides the necessary propulsion to exceed inertia and accelerate the vehicle, $MR(v)$ is the movement resistance as an opposite force to the vehicle movement, $B_e(v)$ is the braking effort used to decelerate the vehicle and stop it permanently (Vukan, 2007).

The traction and braking effort act directly in the vehicle wheels edges. The movement resistance is given by:

$$MR(v) = 10^{-3} \times \left(2.5 + 10^{-3} \times k\left(v + \Delta v\right)^2\right) \times TM \times g \qquad (5)$$

Where $k \approx 0.33$ for passengers' vehicles, $\Delta v \approx 15$km/h is the wind velocity variation, TM is the total mass of the vehicle, and g the gravity. Table 1 presents the action forces in an EMRTS that makes its path between two passengers' stations. As a result, there are four regimens of operation: stopping, acceleration, constant velocity, and deceleration. This is how the difference between the traction effort, the movement resistance, and the braking effort, which are not velocity variants, represent the net force of the vehicle (Jong & Chang, 2005b).

Operative Regimen	Net Force	Velocity
Stopping	$TE(v) - MR(v) - B_e(v)=0$	$v=0$
Acceleration	$TE(v) - MR(v) - B_e(v)>0$	$0 < v < v_{max}$
Constant Velocity	$TE(v) - MR(v) - B_e(v)=0$	$v > 0$
Deceleration	$TE(v) - MR(v) - B_e(v)<0$	$0 < v < v_{max}$

Table 1. Net Force and Velocity as function of the Operative Regimen (Jong & Chang, 2005b)

2.1.2 Computation of dynamic variables

The incremental acceleration (a_i) is obtained from the net force and the total mass of the vehicle (Jong & Chang, 2005b) computed for each instant t, as:

$$a_i(t) = \frac{F(t)}{TM(t)} \tag{6}$$

The velocity is assumed an independent variable, which determines the path time of the traction vehicle, with steps fixed by velocity and acceleration (Jong & Chang, 2005b). So, the time steps and the incremental travelled distance are given by:

$$t_{i+1} = t_i + \frac{v_{i+1} - v_i}{a_i} \tag{7}$$

$$s_{i+1} = s_i + v_i(t_{i+1} - t_i) \tag{8}$$

2.1.3 Power consumption computation

The motor torque and the velocity for an EMRTS are linear functions of the acceleration and the angular velocity. So, the instantaneous power consumption by the EMRTS, for the first three operative states (Chen et al., 1999), (Perrin & Vernard, 1991), (Hsiang & Chen, 2001), is:

$$P(t) = (TM(t) \times a_i(t) + MR(v)) \times v \tag{9}$$

For the last operative state where the braking acts, the consumption is given by:

$$P(t) = B_e(v) \times v \times \eta_B \tag{10}$$

which describes the braking effort multiplied by the velocity in the range of $0 \le v \le v_{max}$ and a multiplicative factor η_B which describes the efficiency of the regenerative braking which it is considered of 30% for this type of systems (Perrin & Vernard, 1991), (Jong & Chang, 2005a), (Hill, 2006).

2.2 Simulation model

The model presented at section 2.1 allows the computation of the power consumption and travel time characteristics (t, x) for each train i in the railway line. Naturally, a railway line simulation must include a number n of passengers' stations and k trains travel in the line (go and return).

The integration of these characteristics requires modelling the mobility of passengers associated at each train. It can be simulated in a probabilistic way, computing the number of passengers coming up and leaving the train (i) in each passenger's station (j) and the stopping time of the train in each station. This first part, stated here as Module 1, uses the following parameters: the passengers' up (r_{up}) and down (r_{down}) rates, and up (t_{up}) and down (t_{up}) times per passenger.

The number of passengers in the first station and the number of passengers waiting in each station (pax_{wait}) are modelled as random variables of uniform distribution. As, the railway line simulation includes a number n of passengers' stations; Module 1 computes for each train i the number of passengers that the train transport between station j and $j+1$ as:

$$pax(i,j) = (1 - r_{down}) \times pax(i,j-1) + pax_{wait}(j) \times r_{up} \tag{11}$$

The number of passengers is constrained to be less or equal than the maximum capacity of passengers at the train. In addition, this module gives the stopping time for each train at each passenger's station ($t_{stop}(i,j)$) based on passengers up and down times, as:

$$t_{stop}(i,j) = t_{down} \times (1 - r_{down}) \times pax(i,j-1) + t_{up} \times pax_{wait}(j) \times r_{up} \tag{12}$$

The second part of the model, called Module 2, simulates the overall travel of train *i*. This means, the simulation gives the power consumption of train *i* for each instant of time *t* for a complete travel (go and return). At the same time, the placement (*x(t)*) of the train is get for each *t*. If the line railway has a length *L*, then the total travel of one train is *2L*, and *x* will be between *0* and *L* in one sense and between *L* and *0* in the another sense.

So, Module 2 computes the train's time of travel between passengers' stations and the instantaneous power demand for one train based on equations (1) to (10) and the number of passengers and stopping time obtained from (11) and (12), respectively; as Fig. 3 shows. As, it is shown, the simulation considers the initial dispatch time and computes the initial value of passengers using the second term of equation (11).
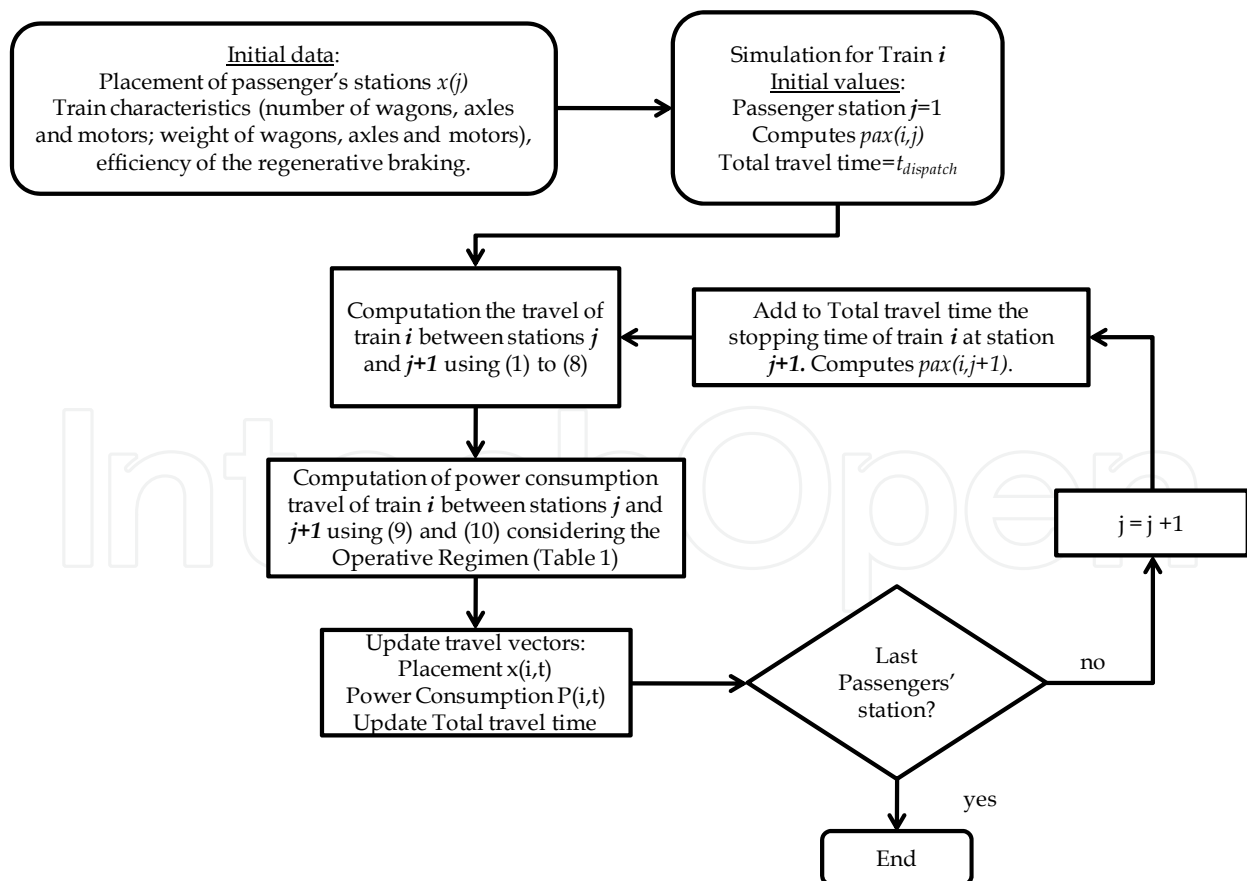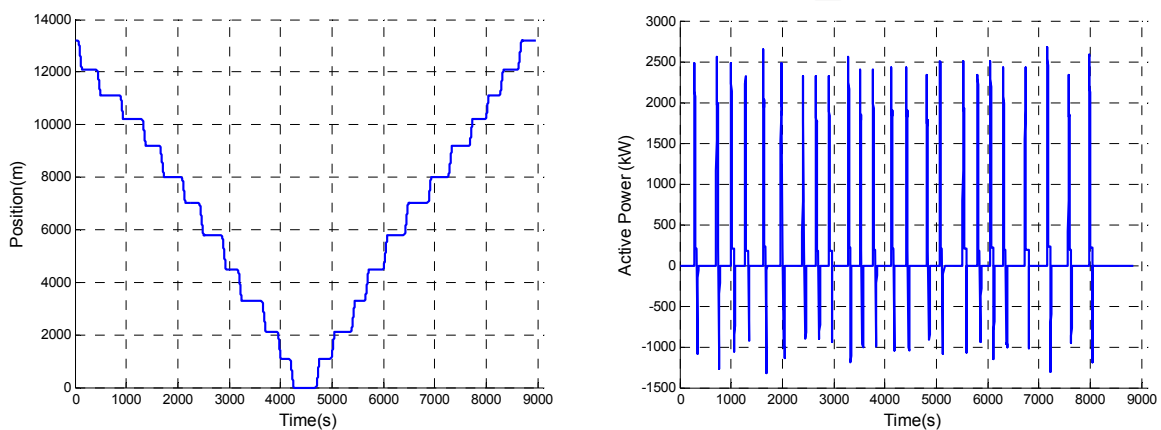

Fig. 3. Simulation of Train *i* Travel – Module 2

On the other hand, Module 2 considers the maximum velocity, the braking and traction effort curves as input variables. These curves are parameterized by means of (1), (2), and (3) and are given by manufacturers of traction equipment. Each curve is used to establish the net force at each operative regime, I to IV in Fig. 2. Fig. 4. shows an example of the simulation of placement and power consumption for a train in a metro line using a power demand simulator reported at (Garcia et al., 2009).

Finally, the simulation of Module 2 is run for the total number of k vehicles in the railway line, taking into account the dispatch time of each one. Then, the power consumption at each TS is computed as Fig. 5. shows. Each TS supplies the power to trains (going or returning) placed for its specific portion of the railway line (the DC section connected to the TS).

a) Graphical Interpretation of x(i,t)   b) Graphical Interpretation of P(i,t)

Fig. 4. Example of Simulation of Train i Travel – Module 2
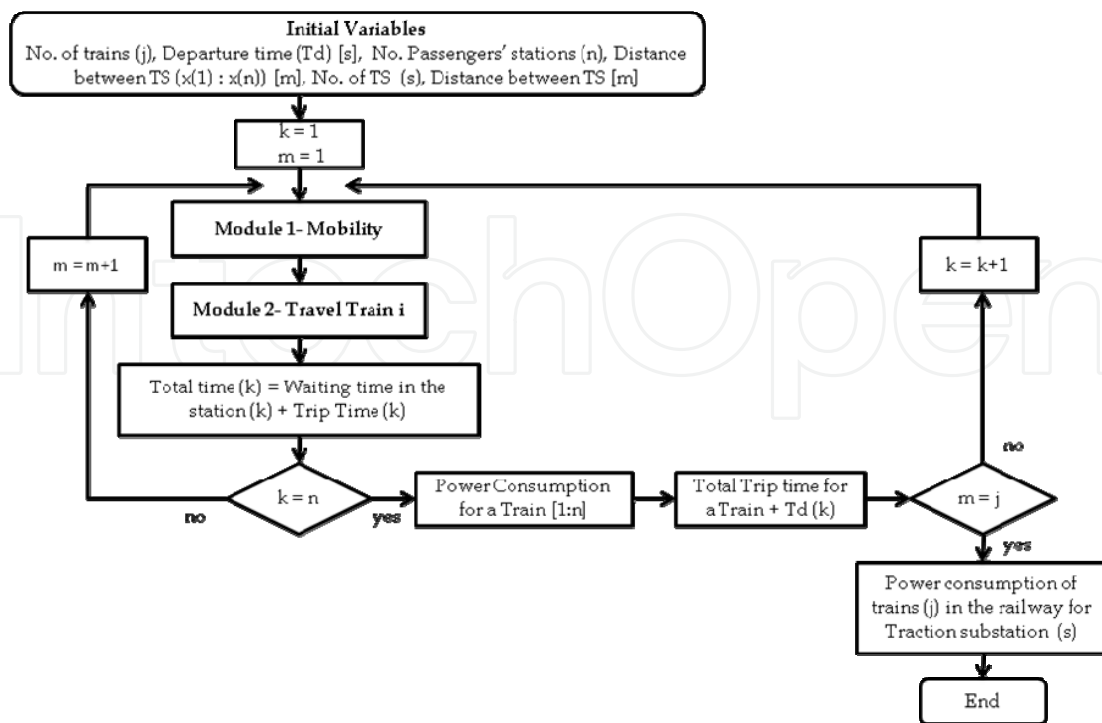

Fig. 5. Simulation of Power Consumption of a Railway Line

2.3 Simulation example

This section illustrates the application of the power consumption mathematical and simulation model in a possible metro line for the city of Bogota of 13.2 km and 13 passenger stations. Fig. 6 shows one section of the possible line 1 to be developed in Bogotá. Fig. 7. presents the results of a simulation of the Metro Line of Fig. 6 using the previous algorithms.
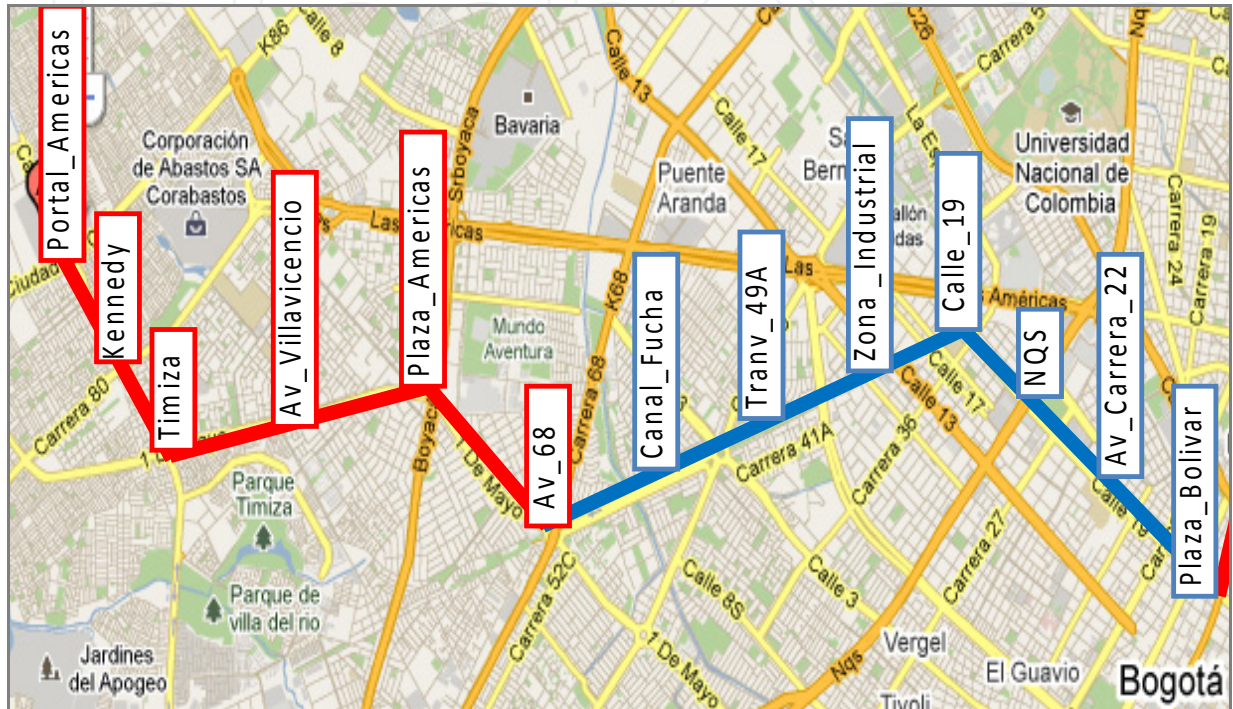

Fig. 6. Example Case of Power Consumption for a Metro Line

a) Train's Trajectories x(i,t)   b) Power Demand P(i,t) substation 1
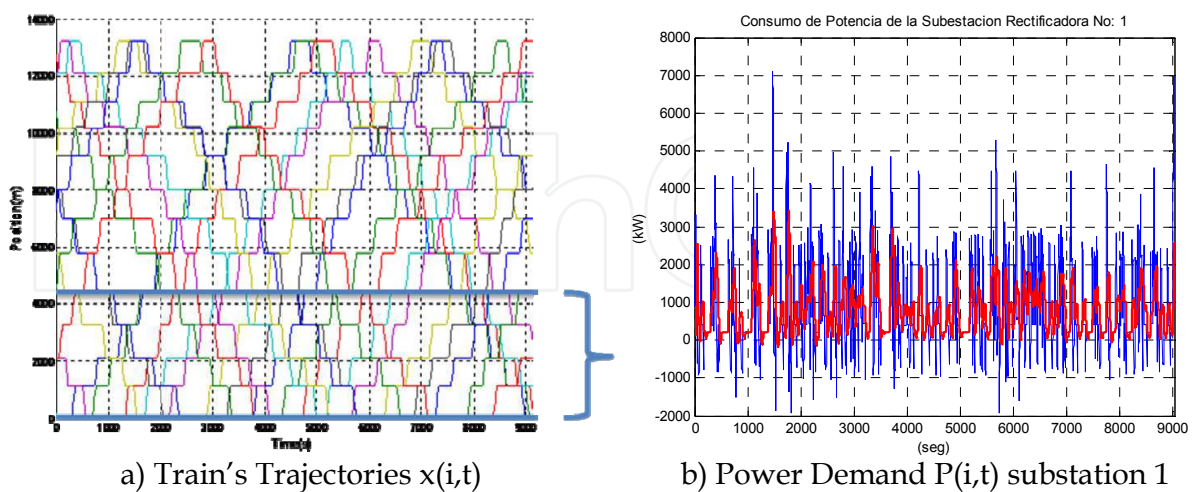
Fig. 7. Power Demand of a Traction Substation – Estimation by Simulation

The simulation establishes the trajectories of 17 trains-vehicles at the Metro Line (Fig. 7.a). The power is supplied by 3 TS. Fig. 7.b shows the power demand at the first traction substation that supplies all trains placed between position 0<x(t)<4400 m.

3. Placement and sizing traction (rectifier) substations in urban railway systems

In this section, a methodology of placement and sizing of traction substations under an electric connection scheme, in which high reliable levels are guaranteed, is presented. In this scheme, each traction substation (TS) is able to support the load of each adjacent substation. That means that in the case when a fault occurs in one TS, there is a support system based on automatic switches normally opened that close and allow the two neighbour substations to supply the power to the associated load with the faulted substation (each one would feed half of the load of the faulted one). The input data to calculate the sizing of substation is obtained from the power demand computation, explained in the previous section.

On the other hand, the placement of each TS is obtained by a heuristic optimization problem. This problem minimizes the total cost of a given configuration, that is composed of investment costs (rectifiers, transformers, and protection and control cells), the cost of energy losses composed by AC losses (associated with the transformer) and DC losses (associated to rectifiers) and the failure cost, that represents the cost of the annual expected energy not supplied (EENS).

3.1 Traction substation (TS) configurations

A scheme of supply of an urban railway system must satisfy electric conditions, such as: operating limits, voltage drops through the catenaries or third rail (called here, in general, DC section), and maximum capacity of transformers. These conditions must be satisfied for supplying the power demand independently of the operating state of the system, i.e., normal state or a post-contingency state after a fault of a HV/MV substation, or TS, or one DC section. So, the TS location and configuration's selection are strongly linked problems. Fig. 8 shows three possible schemes of connection of the MV network to a set of TS. Each TS is designed to supply (in normal operation state) a DC sector of length L.

The way of behave in a fault condition determines the following three possible configurations:

1. **One transformer-rectifier unit with possibility of power supply from the adjacent TS**. Each TS acts as a support of its adjacent TS. This implies that the substations must be able to supply at least 1.5 times the length of the normal DC section length (3L/2).
2. **Two transformer-rectifier units in each traction substation**. This configuration means the redundancy in the main equipment of the TS. In case of a fault in one transformer and/or rectifier, the parallel unit must supply the total power demand of the TS. This scheme assumes that there is not possibility of support of adjacent substations. The wide dotted line if Fig. 8 remarks the parallel unit of transformer-rectifier unit.
3. **Two transformer-rectifier units in each TS and support of adjacent DC section**. This is the combination of configurations 1 and 2. This means that there is redundancy in each traction substation and there is also possibility of support of adjacent DC section feeder.
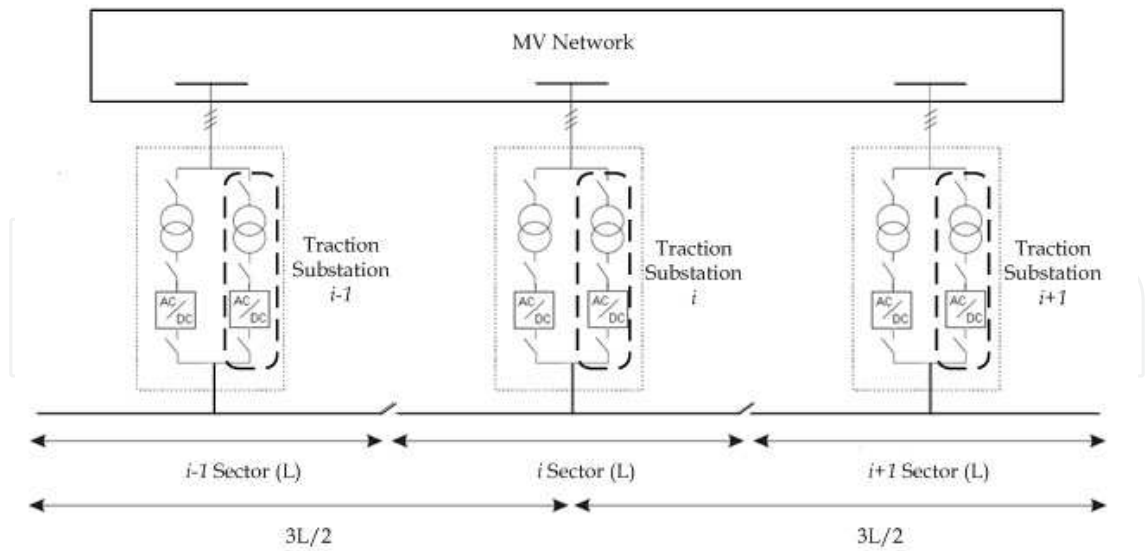
Fig. 8. Configurations of Traction Substations' Connection

3.2 Optimization problem

A minimization of the total project cost is solved for determining the quantity of traction substations, their connection configurations, and their locations. The optimization is a constrained problem that guarantees the electrical requirements, like voltage levels and high reliability requirements. The distance between TS is assumed to be equal, and each TS is located at the middle point of the DC section that it supplies, as Fig. 8 shows.

The cost function (*TC*) includes investment costs, operation costs C_{op} (associated with losses) and reliability cost or cost of energy not supplied (C_{ENS}). So, the total cost for each configuration is given by:

$$TC = C_{inv} + \sum_{j=1}^{T}\left(\frac{C_{op}(j)}{(1+r)^{j}} + \frac{C_{ENS}(j)}{(1+r)^{j}} \right) \qquad (13)$$

Where *T* is the number of years of the project, and *r* is the discount rate of the project. The investment cost depends on the length of the DC network, and is given by:

$$C_{inv} = (L_{cat} \times C_{cat}) + \sum_{i=1}^{m}\left(N_{Mod}(i) \times C_{Mod}(i) + C_{Place}(i) \right) \qquad (14)$$

Where, L_{cat} and C_{cat} are the total length and the unitary cost of the catenaries or rail (DC section, in general). N_{Mod} is the number of modules in one traction substation (1 or 2). C_{Mod} is the cost associated to one module; C_{place} is the cost of the terrain where the substation is built; *m* is the number of substations.

The annual operation cost ($C_{op}(j)$) is computed as the sum of annual AC and DC losses in the year *j* multiplied by the energy cost. Transformer losses are defined as the sum of the instantaneous iron losses ($AC_{iron\text{-}loss}$) and copper losses ($AC_{copper\text{-}loss}$) during the year. Then, the total losses cost for *m* substations is:

$$C_{op}(j) = Cost_{Energy}(j) \times \sum_{i=1}^{m} \left(AC_{loss}(i,j) + DC_{loss}(i,j) \right) \qquad (15)$$

$$AC_{loss}(i,j) = \frac{1}{T_o} \times \int_{0}^{To} \left(AC_{iron-loss}(i,j) + AC_{copper-loss}(i,j,t) \right) dt \qquad (16)$$

T_o is the operation time of the urban rail during the year. The "iron losses" in the transformer are constant (Institution of Electrical and Electronic Engineers [IEEE], 2007) and computed as it is established in (IEEE, 1992). The "copper losses" are directly proportional to the square of the utilization factor (*UF*), and the constant of proportionality is the nominal copper losses of the transformer (P_{nom_Cu}) (IEEE, 2007). The *UF* is defined as the ratio of instantaneous demanded power ($P_{dem}(i,j,t)$) and the transformer rating (P_{nom}).

On the other hand, the DC losses are power losses in the rectifiers (AC/DC converters):

$$AC_{cooper-loss}(i,j,t) = P_{nom\_Cu}(i) \times (UF(j,t))^2 = P_{nom\_Cu}(i) \times \left(\frac{P_{dem}(i,j,t)}{P_{nom}(i)} \right)^2 \qquad (17)$$

$$DC_{loss}(i,j) = \frac{1}{T_o} \times \int_{0}^{To} \left(1 - eff(i,j,t) \right) \times P_{dem}(i,j,t)) dt \qquad (18)$$

The *eff(i,j,t)* is the DC efficiency of the rectifier of the TS *i* and depends on the instantaneous power demanded at year *j* hour *t*. It varies from 95.4% to 95.7% (Hill, 2006).

The third term of the objective function of the minimization problem is the cost of energy not supplied (C_{ENS}), computed as function of the time of no-supply in hours/year (T_{NS}), the unitary cost of fault in USD\$/kWh (C_{fault}) and the average power not supplied by TS (P_{av}):

$$C_{ENS} = T_{NS} \times P_{av} \times C_{fault} \qquad (19)$$

3.3 Technical constraints

The voltage drop between a supply point and a utilization point must not be more than 15% in normal operation and as maximum 30% in special cases (Arriagada & Rudnick, 1994). These specials cases may be the outage of a substation or the last DC section in the route. Table 2 presents the voltage margins according to the different used DC system voltages.

DC system voltage (V)	600	750	1500	3000
Lowest voltage. Undefined duration (V)	400	500	1000	2000
Nominal design system voltage (V)	600	750	1500	3000
Highest voltage. Undefined duration (V)	720	900	1800	3600
Not-permanent highest voltage. Duration of 5 minutes (V)	770*	950**	1950	3900

* In the case of regenerative braking, 800 V is admissible.
** In the case of regenerative braking, 800 V is admissible.

Table 2. Voltages in DC Traction Systems (White, 2009).

A voltage drop of 30% between the TS and the last vehicle can be tolerated in a suburban system, where the vehicles are constantly accelerating, but a voltage drop over the principal line of a *metro* during any time interval might exceed all the established limits. Therefore, the maximum voltage drop allowed is limited to 15% on nominal voltages under normal conditions. A voltage drop in the farthest point of a section supplied by TS is defined as:

$$V_T = V_S - L_2 Z n I - Z_x(n + n')I - \frac{1}{4}(Z n \times I \times LCat(i) - Z \times L_2) \qquad (20)$$

$$Z_x = (R_u + R_T)\cos\phi + (X_u + X_T)\sin\phi \quad and \quad Z = R\cos\phi + X\sin\phi \qquad (21)$$

Where V_s is the DC voltage at the TS (p.u), V_T is the minimum DC voltage in the DC section for correct vehicle operation (p.u.); I is the current demanded by a vehicle (p.u.); R_u and X_u are the equivalent resistance and reactance, respectively (p.u.); R_T and X_T are the transformer resistance and reactance, respectively (p.u.); ϕ is the angle of power factor (zero for DC systems); R and X are the DC section resistance and reactance, including the return way, in p.u./mi; L_2 is the distance between the TS and the nearest vehicle at the right; n and n' are the number of vehicles at the right and the left, respectively, of the TS.

Voltage drop in the farthest point is determined by the maximum length of the sector supplied. In normal conditions, this value is the length L (see Fig. 8). However, when a contingency occurs, the sector length must be modified to almost twice the original length. Then, for normal conditions, the voltage must satisfy:

$$V_T \le V_S(i) - Z(i, L/2) \times I_{TS}(i) \qquad (22)$$

Where I_{TS} is the current delivered by the TS depending on the number of vehicles in sector i supplied in a determined time by the substation. Under a contingency of the TS, the voltage must satisfy the constraint for the sector i-1 and sector i+1 (adjacent sectors):

$$V_T(i \pm 1) \le V_S(i \pm 1) - Z(i \pm 1, 3L/2) \times I_{TS}(i \pm 1) \qquad (23)$$

The minimum capacity of transformers and rectifiers is calculated from the maximum demanded current in each TS. The transformers and rectifiers size must be chosen as the nearest superior value to the demanded power, depending on the commercial capacities. As previously, normal conditions and post-contingency operation must be considered. In normal operation with 2 transformers, the power capacity of transformers must satisfy:

$$CapT(MW)(i) \ge I_{TS}(i, L) \times V_{DC} + P_{Loss}(L) \qquad (24)$$

Meanwhile, when the traction substation i is unavailable, the capacity of active power of the 2 transformers in the i-1 and i+1 sector must satisfy:

$$CapT(MW)(i \pm 1) \ge I_{TS}(i \pm 1, 3L/2) \times V_{DC} + P_{Loss}(3L/2) \qquad (25)$$

The capacity in MVA of the transformer is computed dividing the capacity in MW by the power factor (p.f.). As shown in (24) and (25), the power loss (P_{loss}) in the DC section feeder for the maximum demand must be determined for each section. The total power loss in DC section associated to the TS for a round trip is:

$$P_{LOSS} = \sum_{t=0}^{To} P_{loss}(t) = \sum_{t=0}^{To} \left[\sum_{j=1}^{n'} I_j(t)^2 \times \rho \times L_j(t) + \sum_{j=1}^{n} I_j(t)^2 \times \rho \times L_j(t) \right] \qquad (26)$$

I_j is the current in each DC section that is defined as the catenaries/rail between two vehicles or between a vehicle and the TS (in the case of the nearest vehicle to the feeding point of the TS). The total losses at the DC section takes into account all vehicles placed at left and right of the TS. ρ is the resistivity of the DC section [Ω/km or Ω/mi]; T_o is the total annual operation time.

3.4 Application to the study case

The analysis was developed for the metro line showed in Fig. 6 corresponding to the study case of section 2.3. The study was developed as function of the number of substations and the three possible configurations explained in section 3.1.

The unitary cost of fault was assumed 1074 US$/kWh, from reliability analysis. Simulations were done for three levels of load: high (the maximum number of vehicles in service), medium (half of the total vehicles in service), and low (with no vehicles in service). The simulator allows the calculation of power losses in N-0 state, and the demand of each substation for N-0 and N-1 contingencies state.

Simple contingencies (N-1) at the maximum load were made in order to sizing the TS when configurations 1 and 3 are used, to give support of adjacent TS. While, normal state operation was used for sizing TS in configuration 2.

Table 3 presents the total cost computed as function of the number of TS and configuration of connection. Additionally, the investment cost (C_inv) and the net present value of the operation cost (NPV_Oper) is shown. The fault cost was of 155.000 USD$/year.

The investment cost (without the cost of catenaries/rail that is common for all alternatives), noted C_inv, includes the switchgear in SF6, rectifiers, transformers, having into account the number of each equipment depending on the configuration (see Fig. 8). The NPV_Oper includes the operation cost for a useful life of the project of 20 years.

In the second column, in brackets, the rating commercial capacity of each substation is shown, based on the results of simulations and the algorithm for finding catenaries/rail losses. The capacities of each substation for configurations 1 and 3 are the same, due to the high electrical similitude between both schemes.

#TS's	Configuration (rating/TS)	Maximum length of catenary/rail (km)	Millions of dollars		
			C_inv	NPV_Oper	Total Cost
3	1 (5MW)	8.8	6.11	0.81	7.95
	2 (4 MW)	4.4	9.75	1.63	12.4
	3 (5MW)	8.8	11.9	1.62	14.5
4	1 (5 MW)	6.6	6.73	0.90	8.65
	2 (3.75MW)	3.3	12.3	1.79	15.1
	3 (5 MW)	6.6	13.0	1.79	15.8
5	1 (3.75MW)	5.28	7.97	0.98	9.97
	2 (3.75MW)	2.64	14.3	1.97	17.3
	3 (3.75MW)	5.28	15.4	1.96	18.3

Table 3. Cost Comparison of Several Configuration of TS's Connections – Study Case

The third column shows the maximum length of the DC section that each TS can supply. TS in configurations 1 and 3 must have a capacity to supply even twice the total length of the line divided by the number of considered substations. Instead, TS in configuration 2 supply the maximum length of catenaries/rail, just the normal operation length because this configuration is not able of supporting of adjacent substation in case of fault.

The lowest total cost at Table 3 is presented in the case of three 5 MW TS because, in the study case of section 2.3, the investment cost weights more in the final cost than the operation cost. That is, looking just the configuration 1, it is evident that even though the operation costs do not grow up linearly as more TS are considered, the difference between investment costs is higher than operation costs, so the optimal solution is the location of 3 TS of 5 MW, under the configuration 1.

4. Power quality impact of urban railway systems on distribution systems

Power quality phenomena originated in power distribution systems impacts on the electrical power supply system of UMTS and, at the same time, power electronics used in the traction system impacts on the power quality (PQ) service of the distribution system.

In addition, the power demand of UMTS presents high and fast variations as consequence of the operation cycles of each train-vehicle and the non-coincidence of operational cycles among several vehicles. So, PQ phenomena are time variable (Singh et al., 2006).

4.1 PQ Phenomena and railways' electrical system components

Fig. 9 shows the existing relationships between the different PQ phenomena and the railways' electrical system components. As it is shown, the main electrical components in the railway system are: the train-vehicle as an electric load that involves a great use of power electronics, rectifier substations, the electric HV/MV substation, and the distribution network system (White, 2008).

On the other hand, the main PQ phenomena involved in the interaction between the railways' electrical systems and the power distribution system are: electromagnetic interference (EMI/RFI) at high frequency (HF); harmonics, flicker, and voltage regulation at low frequency (LF) (Sutherland et al., 2006). Also, PQ phenomena include sags at instantaneous regime, unbalance of the three-phase power system, and transients' phenomena (Lamedica et al., 2004).

Fig. 9 (Garcia & Rios, 2010) presents also where the cause of the phenomena is, what are the affected or perturbed systems, and where a solution of the problem can be implemented. For example, the electromagnetic transients occur in microseconds and they are caused by capacitor switching or lightning. Hence, they can be generated in the distribution network, MV side of the rectifier substation or in the train (represented by X in Fig. 9). The main problems are related to the rectifier substation or the train (represented by circle in Fig. 10) where the electronic sensitive equipment are susceptible to misuse or damage due to the transient overvoltage. An effective overvoltage transient protection could be located at the rectifier substation and, finally, at the train (represented by triangle Fig. 9).
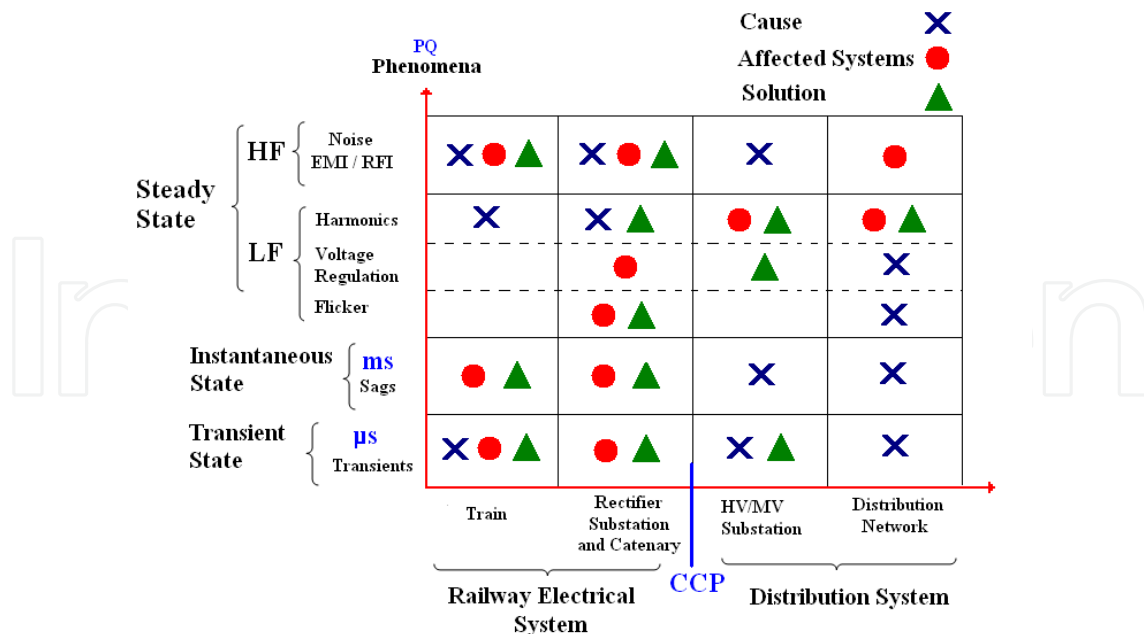
Fig. 9. PQ Phenomena and Railways' Electrical System Components Relationships

4.2 Harmonic distortion analysis

The identification of PQ problems in power systems represents an important issue to the distribution utilities. The harmonic distortion is one of the main PQ phenomena in the electrical system feeding an EMRTS because the injection of harmonics by its nonlinear loads flows through the network and affects other consumers connected to the distribution system. According to the conceptual diagram of Fig. 9, the production of harmonics in the EMRTS is a PQ phenomenon at steady state caused by the rectifier substations, normally, a controlled rectifier of 6 or 12 pluses.

In addition, the computation of the total harmonic distortion (THD) in the AC side of the rectifier substation at the railway system must take into account the time load variability at each TS. So, the instantaneous power load must be computed as function of time and distance as it was explained at section 2. Once the current consumption in each TS is obtained, it is possible to identify the variation of the THD during the time.

4.2.1 Probabilistic model

Generally, deterministic models have been adopted for network harmonic analysis; however, these models can fail for modelling the load variation in systems such as the railways' electrical system (Chang et al., 2009). So, a probabilistic analysis to characterize the harmonic current loads properly must be used in order to obtain an accurate model.

An EMRTS is characterized by fluctuating loads due to the different operation states of the trains in the traction system (See Fig. 7 b). Thus, the harmonics injection from the rectifier substations to the MV network causes that the current harmonic spectrum at the distribution system's connection point (PCC) varies over time. So, each traction substation can be represented as a harmonic current source that provides a probabilistic spectral content at the PCC (Rios et al., 2009).

Then, it is necessary to perform the vector sum of several harmonic sources (i.e. traction substations) at the distribution system's connection point to determine the total harmonic distortion. There are two methods to evaluate the effect of different non-linear loads: the analytical method and Monte Carlo simulation method. The complex implementation of analytical methods for large power systems studies involves little practical application in real systems. By contrast, Monte Carlo simulation has proved to be a practical technique (Casteren & Groeman, 2009) based on the low correlation between different harmonic loads (independence of the sources). Fig. 10 presents the methodology useful for probabilistic harmonic distortion analysis of railways' electrical systems with different harmonic sources.

The methodology for probabilistic analysis of harmonic starts from values obtained from deterministic simulations. Once the different conditions of loads are defined in the behaviour of the traction system, it is possible to use probability distribution plots to evaluate the harmonic level in the system during the travel time. So, the next step is to determine the probability density function to fit the harmonic components of each harmonic source and its phase angle.
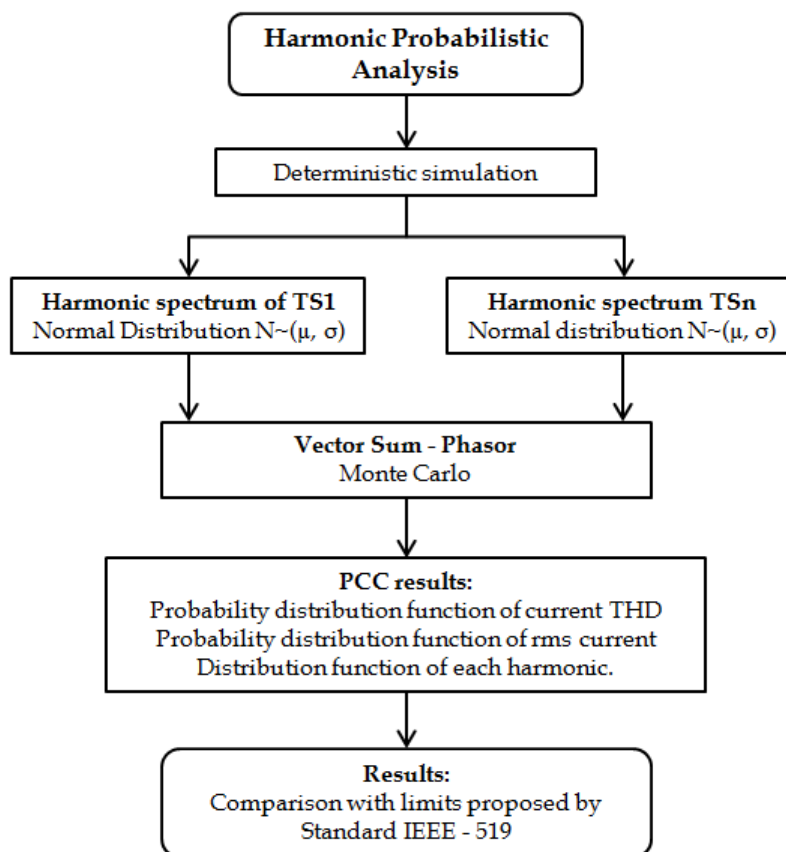

Fig. 10. Methodology for Harmonic Distortion Probabilistic Analysis of EMRTS

Many studies agree that the normal function is suitable as probability density function to use in the case of a random behaviour (Wang et al., 1994). In addition, according to the Std. IEEE - 519 (IEEE, 1993) the recommended window time to evaluate the harmonic distortion is 15 or 30 minutes. Therefore, it is recommended the selection of random time intervals of 15 minutes to make a probabilistic characterization of the THD distortion.

Then, a process called "Vector Sum - Phasor" is run through Monte Carlo simulations. Finally, the probabilistic characterization is obtained; where the probability distribution function of current THD, the probability distribution function of rms current and the probability distribution of each harmonic component are obtained.

Table 10.3 of Std. IEEE - 519 (IEEE, 1993) contains the current distortion limits in the voltage range of 120 V to 69 kV, which applies for typical railways' electrical systems connected to distribution systems at MV. So, based on this standard, a comparison between the current distortion levels at 95% and 50% of probability and the given limits must be realized to assess if the current distortion must be reduced or not. If a current THD distortion must be reduced, it could be used several filters methods. The next section presents the application of active power filtering to reduce THD distortion.

4.2.2 Active power filter allocation methodology

The harmonic distortion produced by railways' systems at the distribution system's connection point can be reduced using passive or active power filters (APF). However, due to the random and time variability of the harmonic distortion in traction systems, it is required an active power compensation with the ability of adaptation to different load conditions. Passive filters are designed with fixed parameters and for specific harmonics, so this type of filter does not have the required ability. By contrast, APFs based on the p-q theory became an effective solution in traction systems; normally, they are used for dynamic harmonic suppression (Xu & Chen, 2009). This type of compensation presents the advantage of eliminating a wide range of harmonics simultaneously.

On the other hand, the traction system has several rectifier substations and from the economic point of view it is difficult to install an APF in each TS due to its high cost. Then, it is necessary to allocate APFs in the most sensitive positions in the own power system of the EMRTS using the least number of filters and minimizing their size. An important factor to be considered in the decision of harmonic compensation in traction system is the sudden fluctuation of traction load because this dynamic behavior is also observed in the harmonic distortion, as it has been explained in the previous section.

The allocation methodology of APFs in distribution systems supplying a traction load is based on probabilistic data of harmonic distortion presented in all traction substations. According to the Std. IEEE - 519 (IEEE, 1993), using a 15 minutes time interval it is enough to understand the dynamic behavior of the traction load because in this interval there are 900 different data of the load behaviour in each TS. Fig. 11 shows the proposed methodology of allocation of APF in urban railways systems.

As, it was shown in section 3.4, for the study case of this Chapter, the metro line can be supplied by three TS at MV. The total harmonic distortion in the distribution system is analyzed with and without active compensation. The APF is allocated in the low voltage side of the transformer in the TS. As, the railway line has three TS, there are seven possible allocations of APF, as Table 4 shows at the first column.

Table 4 shows the THD distortion at levels of 50% and 95% of probability when the system is without active power compensation and when APFs compensation is used according to the seven different configurations. This table shows the effectiveness of the APFs to reduce

the current THD distortion. Although the reduction is achieved with one filter, the amount of reduction is low because the two rectifier substations without active power filter present high variability and distortion. It is also observed that when an additional filter is used the amount of reduction in the THD is higher. Obviously, if three APF are used (one at each TS), the higher THD reduction is obtained.
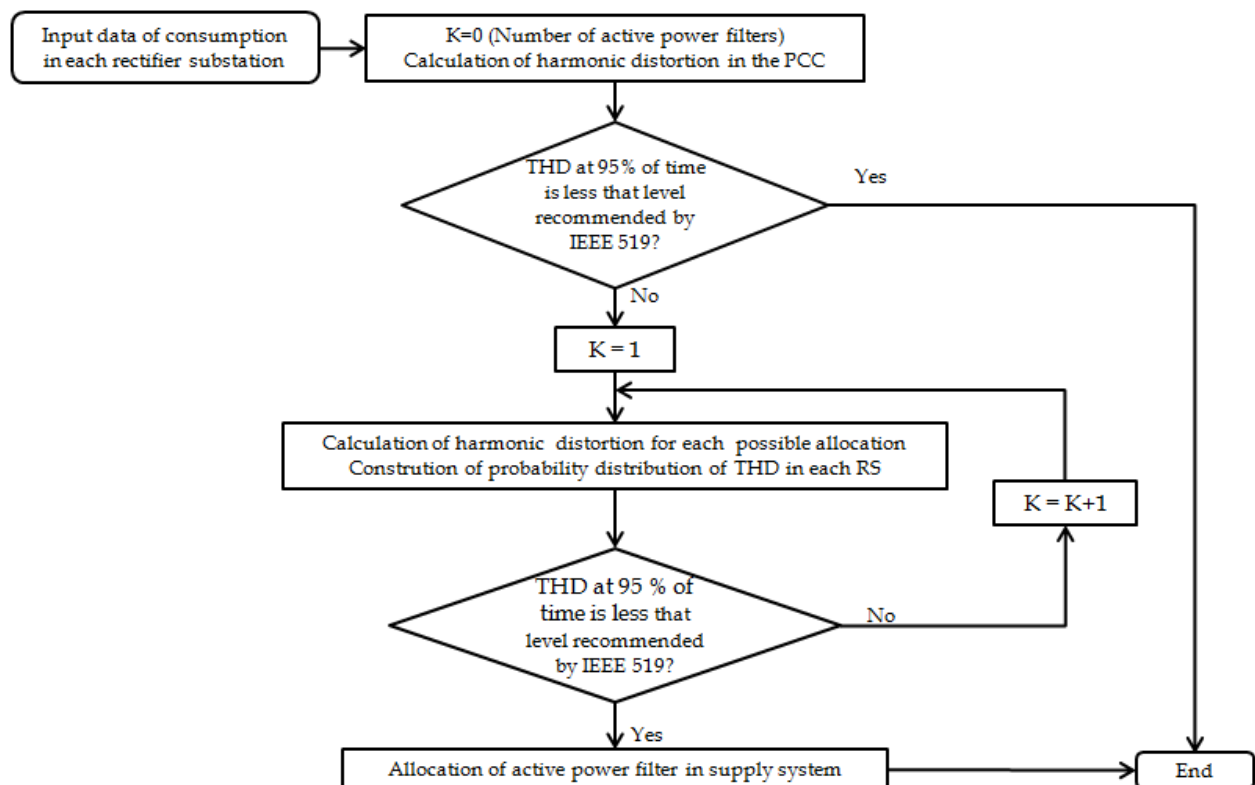

Fig. 11. Methodology for Allocation of Active Power Filters in Urban Railway Systems

The final decision about what configuration selects depends on the short circuit level of the system; for example, if the short circuit level is lower than 50 MVA a placement of one APF at each TS is required to satisfy Std. IEEE-519. By contrast, if the short circuit level is between 50 and 100 MVA, the best option is to place APF at TS1 and TS2.

Case	MEAN THD (%)		THD of 95% of time (%)	
	SUPPLY 1	SUPPLY 2	SUPPLY 1	SUPPLY 2
Without filter	22.96	22.98	23.66	23.66
APF in TS1	14.59	14.84	19.31	19.25
APF in TS2	13.81	13.82	18.94	18.94
APF in TS3	13.75	13.50	17.80	17.77
APF in TS1 and TS2	3.64	3.69	5.44	5.56
APF in TS1 and TS3	3.81	3.82	5.21	5.17
APF in TS2 and TS3	3.68	3.64	5.18	5.06
APF in all TS	3.01	3.00	3.60	3.59

Table 4. Total Current Harmonic Distortion – Active Power Filter Allocation

5. Grounding in DC urban railway systems

A primary requirement to ensure the appropriate operation of any electrical system is to guarantee personnel and system safety, either under normal and fault conditions. So, grounding is the most important component to control electrical system failures.

Grounding in electric traction systems requires a different treatment than in typical AC electrical systems, because of the existence of traction substations AC/DC of high capacity, the high variable load characteristic in time and distance, the direct contact of the rails with the earth, the current flow through the ground during normal operating conditions that can cause corrosion of underground metallic elements, the appearance of step and touch voltage that can jeopardize the integrity of persons.

The grounding system is composed by two subsystems. The first one (subsystem 1) assures the personnel safety and the protective device operation; while, the second one (subsystem 2) is used to ground the negative pole in the DC side of the railway's traction substation.

The grounding subsystem 1 is used to ground all metallic structures: boxes, protective panels, pipeline, bridges, passenger platforms, etc. There are two ways to connect this subsystem:

- High Resistance Grounding Method (HRGM): A constant voltage of 25 Vdc is applied between the TS's housing and the ground, in order to energize a relay to send the opening order to the protection equipment. When the voltage level decreases, other relay is set to send the opening order to the protection if a big current flows through the module. This path is supplied with a resistance of 500 Ω.
- Low Resistance Grounding Method (LRGM): A constant voltage of 1 Vdc is applied between the TS's housing and the ground. In this case no resistance is used, but a direct connection is made to the ground system. In addition, when the relays and protections detect the voltage's absence, they will send the opening order to the protection system.

So, Table 5 presents a comparison of the performance of these two methods.

Technical Features Description	HRGM	LRGM
Monitor constant voltage	25 Vdc	1 Vdc
Relay circuit resistance	High (200-700 Ω)	Low (< 1 Ω)
Current fault-ground structure	Low (1-2 A)	High (70-1500 A)

Table 5. Comparison of HRMG and LRMG performance.

The second subsystem is used to ground the negative conductor of the TS (Paul, 2002) (Lee & Wang, 2001) which corresponds physically to running rails. In DC traction systems, the rails are used as return conductor current, which could cause corrosion problems in underground metallic structures. There are three options to connect this subsystem:

- Solid-grounded system: This system keeps under control touch voltage but it permits the corrosion of the elements grounded to the earth.
- Ungrounded system (Floating): This system keeps under control stray currents but it permits high touch and step voltages.

- Diode-grounded system: Its purpose is to maintain the system without grounding while operating conditions are normal. But in the case of a failure, it quickly makes a change that provides a physical connection between the negative pole and grounding. When it returns to normal conditions, connection with grounding is suppressed. The diode is able to perform this function, as it is complemented by a security relay. The disadvantage is that under normal operating conditions small voltage differences may occur between the negative pole and grounding, forcing the diode to enter in function mode which increases stray currents and their associated effects.

Table 6 compares the main characteristics of the three options of railway's grounding system.

Grounding method	Riel to ground voltage (Vehicle touch voltage)	Stray current level
Solid-grounded system	Low	High
Ungrounded system (Floating)	High	Low
Diode-grounded system	Middle-Low	Middle-High

Table 6. Comparison of the Railway's Grounding Systems

5.1 Generalized grounding model in DC to EMRTS

Fig. 12 illustrates a grounded scheme for a railway line, in which for general purposes there are k trains, m substations and a total rail length *l*.
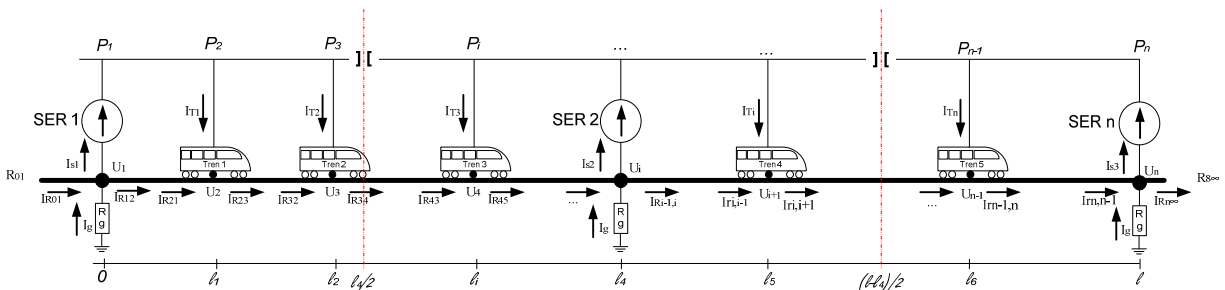

Fig. 12. Grounded System – General Scheme

The behavior of the current and voltage on the rail for each section between points P_i and P_{i+1} for i = 1, 2, 3…, n, is modeled by:

$$I_{Ri,i+1}(x) = c_{(2xi-1)}e^{\gamma x} + c_{(2xi)}e^{-\gamma x} \qquad (27)$$

$$U_i(x) = -R_0(c_{(2xi-1)}e^{\gamma x} - c_{(2xi)}e^{-\gamma x}) \qquad (28)$$

For $0 \leq x \leq l$, where *n* is equal to the number of trains running (*k*) plus the number of TS that are in operation (m), n = k + m. $U_i(x)$ is the rail to ground potential [V], and $I_{Ri,i+1}(x)$ is the stray current in the rail conductor [A].

The constant values $c_{(2xi-1)}$ and $c_{(2xi)}$ can be determined from the solution of a linear system of $2x(n-1)$ equations with $2x(n-1)$ unknowns obtained from the boundary conditions of each point P_i applying Kirchhoff's laws and assuming that the magnitudes of the currents

delivered or absorbed by the trains and the substations are known as well as the location of each of the trains at the moment that these currents are delivered. Different scenarios can arise during the operation, which can be described as: railway starting point (P_1); railway ending point (P_n); point where a train is passing (P_2, P_3, P_4, ... , P_{n-1}); and point where a traction substation is located, for example (P_i).

5.2 DC grounding algorithm model in time

The model uses information on the train location and current consumption or delivered by the traction substations, for all time t. The power demand simulator (section 2) gives the power consumed and delivered by each train and TS, as well as the location of each train along the rail for each time instant. Fig. 13 shows the flowchart of the algorithm.
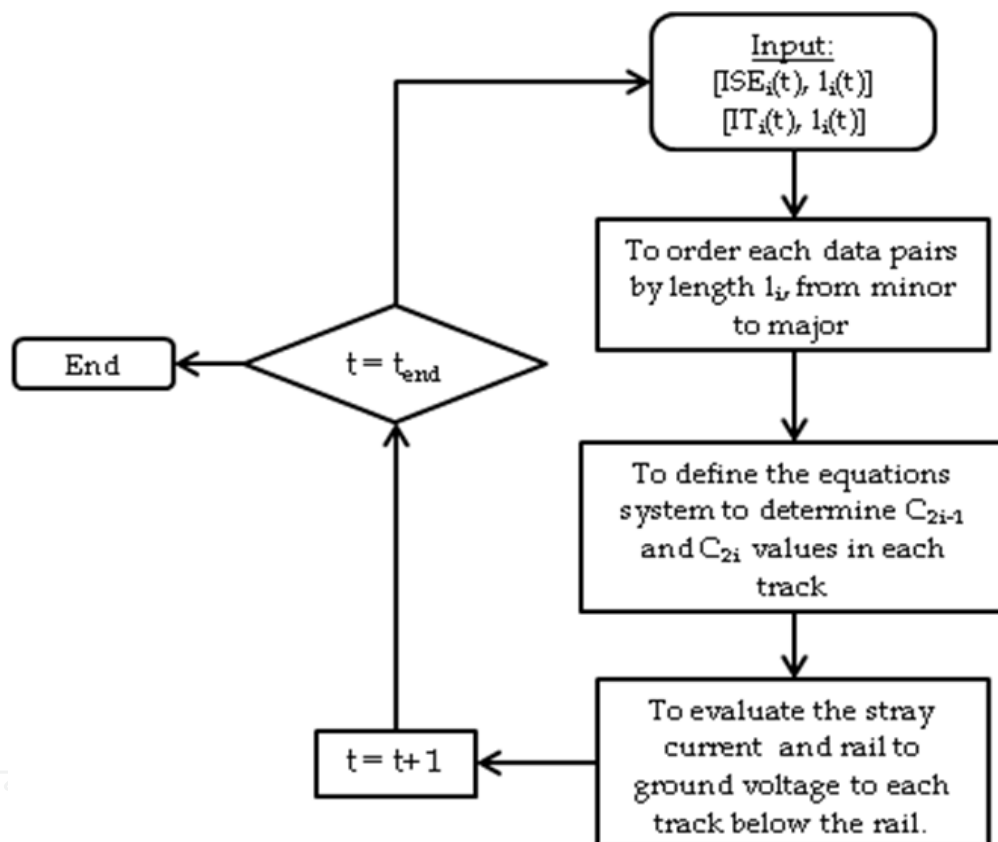
Fig. 13. DC Grounding Algorithm Model in Time

This algorithm has the following characteristics:

- The input data consist of arrays of pairs with the current supplied or absorbed by each TS or train and the respective train locations. This information is supplied by the model presented in section 2.
- As the trains are in constant motion the input for each instant of time is ordered from minor to major, in accordance to their location to the starting point of the track, in order to determine the track to be evaluated.
- After defining the tracks and points (P_i) on the total rail length, values are determined for each constant $c_{(2xi-1)}$ and $c_{(2xi)}$ respectively.

- Finally, using the constants obtained in the previous step for the instant of time the stray current and the voltage rail to ground are evaluated and the information obtained is saved. This process is repeated from the second step until all points in time.

5.3 Example

Let us consider a simplified study case similar to the system of section 2.3 (Fig. 6) with three TS located at 0, 2000 and 4000 meters and four trains moving along the 4 kilometers of rail. Constant system parameters are: R=0.04Ω/km, G=0.1S/km, R_g=0.01Ω/km and R_{01}=$R_{8\infty}$=R_0.

a) Currents at Trains   b) Currents at Traction Substation
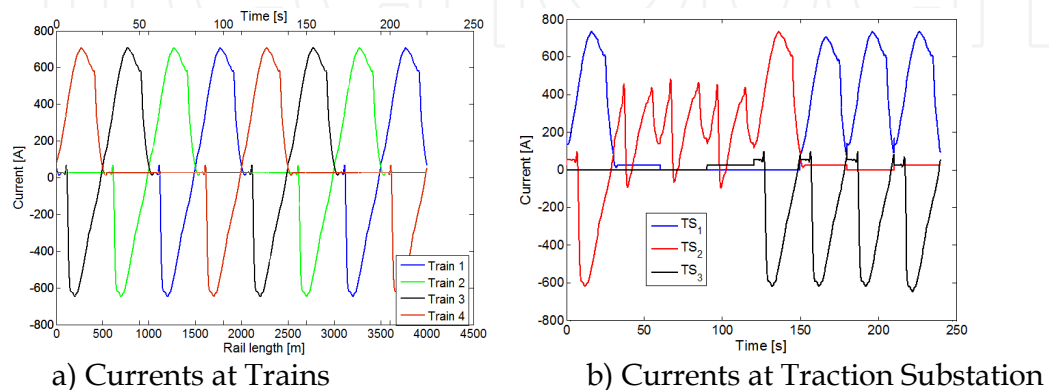
Fig. 14. Example of Simulation of Grounding

Fig. 14a shows the current magnitude of each train and its location on the rail for each moment. Likewise, Fig. 14b shows the current magnitude in each traction substations for each time instant.

Fig. 15 shows the voltage profile along of the rail length at different points in time obtained from the simulation for the case of diode-grounded system. With this system, it is possible to reduce the voltage difference presented in the ungrounded system as the solid-grounded system behaviour. The simulations results show that the diode-grounded system guarantees greater security because it control the step and touch voltage and reduces the stray currents that cause the deterioration of the physical installation.
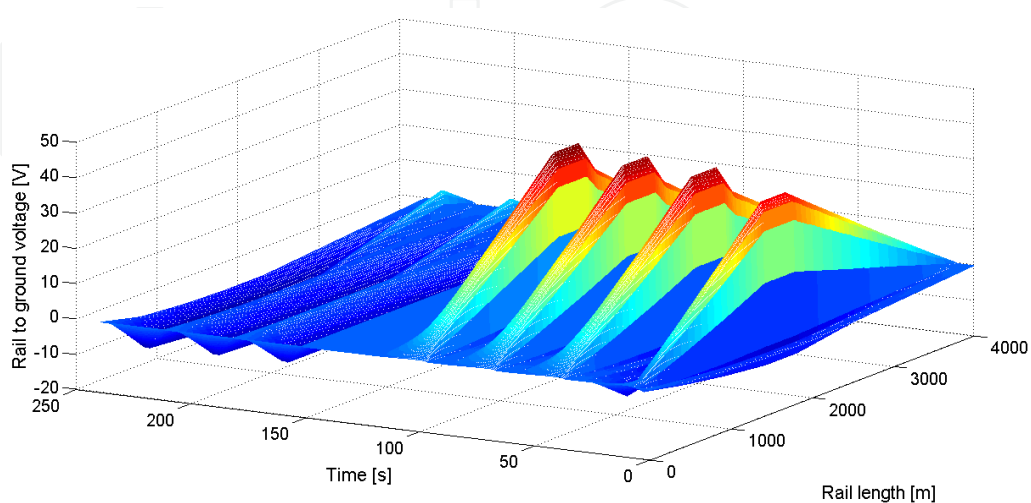

Fig. 15. Rail to Ground Time Voltage Profile

6. Conclusion

This chapter has presented useful tools for power systems modelling, analysis and system design of Electric Massive Railway Transportation Systems (EMRTS) and power supply from Distribution Companies (DisCo) or Electric Power Utilities. Firstly, a section depicted to present the modelling and simulation of the power demand was developed. Then, a section about the computation of the placement and sizing of traction substations for urban railway systems was presented where the modelling is based on the power demand model of the previously mentioned.

After that, two sections about the power quality impact of EMRTS on distribution systems and grounding design are presented. Both subjects make use of the load demand model presented at section 2.

These tools allow the optimization of the design scheme of railway electrification for UMTS, taking into account an adequate sizing and number of traction substations, and the number and location of harmonic filters to improve the power quality of the system.

7. Acknowledgment

8. References

Arriagada, A.; & Rudnick, H. (1994). *Reliability Evaluation in Electric Distribution Systems* (in spanish). Escuela de Ingeniería, Pontificia Universidad Católica de Chile.

Buhrkall, L. (2006). Traction System Case Study, In: *Electric Traction Systems*, IET (Ed.), pp. 53-71, ISBN 978-0-86341-9485, London, UK.

Casteren, J.V.; Groeman, F. (2006). Harmonic analysis of rail transportation systems with probabilistic techniques, *9th International Conference on Probabilistic Methods Applied to Power Systems*, ISBN 978-91-7178-585-5, Stockholm, Sweden, June 11-15, 2006.

Chang, G.W.; Hung-Lu, W.; Gen-Sheng, C.; Shou-Yung, C. (2009). Passive harmonic filter planning in a power system with considering probabilistic constraints, *IEEE Transactions on Power Delivery*, Vol. 24, No.1, (Jan. 2009), pp. 208-218, ISSN 0885-8977.

Chen, C.S.; Chuang, H.J.; & Chen, J.L. (1999). Analysis of dynamic load behavior for electrified mass rapid transit systems, *34th IEEE Industry Applications Conference*, Vol. 2, pp. 992-998, ISBN: 0-7803-5589-X, Phoenix, Arizona, USA, October 3-7, 1999.

Garcia, J.G.; Ríos, M.A.; Ramos, G. (2009). A power demand simulator of electric transportation systems for distribution utilities, *44th International Universities Power Engineering Conference UPEC 2009*, ISBN 978-1-4244-6823-2, Glasgow, Scotland, September 1-4, 2009.

Garcia, J.G.; Rios, M.A. (2010). PQ analysis in tramway systems, *2010 IEEE ANDESCON*, ISBN 978-1-4244-6740-2, Bogotá, Colombia, 15-17 Sept., 2010.

Hill, R.J. (2006). DC and AC Traction Motors, In: *Electric Traction Systems*, IET (Ed.), 33-52, ISBN 978-0-86341-9485, London, UK.

Hsiang, P.; & Chen, S. (2001). Electric Load Estimation Techniques for High-Speed Railway (HSR) Traction Power Systems, *IEEE Transactions on Vehicular Technology*, Vol. 50, No. 5, (September 2001), pp. 1260-1266, ISSN 0018-9545.

IEEE (1992). IEEE Loss Evaluation Guide for Power Transformers and Reactors, IEEE (ed.), ISBN 1-55937-245-1, New York, USA.

IEEE (1993). IEEE recommended practices and requirements for harmonic control in electrical power systems Standard 519 – 1992, IEEE (ed.), ISBN 1-55937-239-7, New York, USA.

IEEE (2007). IEEE standard general requirements for liquid-immersed distribution, power, and regulating transformers C57.12.00-2006, IEEE(ed.), ISBN 0-7381-5251-X, New York, USA.

Jong, JC..; & Chang, S. (2005a). Models for Estimating Energy Consumption of Electric Trains, *Journal of the Eastern Asia Society for Transportation Studies*, Vol. 6, (2005), pp. 278 - 291, ISSN 1881-1124.

Jong, J.C.; & Chang, S. (2005b). Algorithms for Generating Train Speed Profiles, *Journal of the Eastern Asia Society for Transportation Studies*, Vol. 6, (2005), pp. 356 - 371, ISSN 1881-1124.

Lamedica, R.; Maranzano, G.; Marzinotto, M.; & Prudenzi, A. (2004). Power quality disturbance in power supply system of the subway of Rome, *IEEE Power Engineering Society General Meeting*, pp. 924 – 929, ISBN 0-7803-8465-2, Denver, USA, 6-10 June, 2004.

Lee, C.H.; Wang, H.M. (2001). Effects of Grounding Schemes on Rail Potential and Stray Currents in Taipei Rail Transit Systems, *IEE Proceedings on Electric Power Applications*, Vol. 148, No. 2, (Mar. 2001), pp. 148–154, ISSN 1350-2352.

Paul, D. (2002). DC traction power system grounding, *IEEE Transactions on Industry Applications*, Vol. 38, No.3, (May/Jun 2002), pp. 818 - 824, ISSN 0093-9994.

Perrin, J.P.; & Vernard, C. (1991). *Urban Electric Transportations* (in French), D5-554 Techniques de l'Ingénieur, France.

Rios, M.A.; Ramos, G.; Moreno, R. (2009). Evaluación de Calidad de la Potencia en la Interacción del Sistema de Distribución y los Sistemas Eléctricos Ferroviarios Urbanos, *8th Latin-American Congress on Electricity Generation and Transmission CLAGTEE*, ISBN 978-85-61065-01-0, Ubatuba, Brazil, October 18-22, 2009.

Singh, B.; Bhuvaneswari, G.; & Garg, V. (2006). Improved power quality AC-DC converter for electric multiple units in electric traction, *2006 IEEE Power India Conference*, ISBN 0-7803-9525-5, New Delhi, India, 2006.

Sutherland, P.; Waclawiak, M.; & McGranaghan, M. (2006). Harmonic Impacts Evaluation for Single-Phase Traction Load, *International Journal on Energy Technology and Policy*, Vol. 4, No. 1, (2006), pp. 37-59, ISSN 1472-8923.

Vukan, R. (2007). *Urban Transit Systems and Technology*, John Wiley & Sons, Inc., ISBN 978-0471758235, NJ, USA.

Xu, X.; Chen, B. (2009). Research on Power Quality Control for Railway Traction Power Supply System, *Pacific-Asia Conference on Circuits, Communications and Systems*, ISBN 978-0-7695-3614-9, Chengdu, China, May 16-17, 2009.

Wang, Y.J.; Pierrat, L.; Wang, L. (1994), Summation of harmonic currents produced by AC/DC static power converters with randomly fluctuations loads, *IEEE Transactions on Power Delivery*, Vol. 9, No. 2, (April, 1994), pp. 1129 – 1135, ISSN 0885-8977.

White, R.D. (2008). AC/DC railway electrification and protection, In: *2008 IET professional development course on Electric Traction Systems*, IET (ed.), pp. 258 – 305, ISBN 978-0-86341-948-5, UK.

White, R.D. (2009). DC electrification supply system design, In: *4th IET professional development course on Railway Electrification Infrastructure and Systems*, IET (ed.), 44–69, ISBN 978-1-84919-133-3, UK.
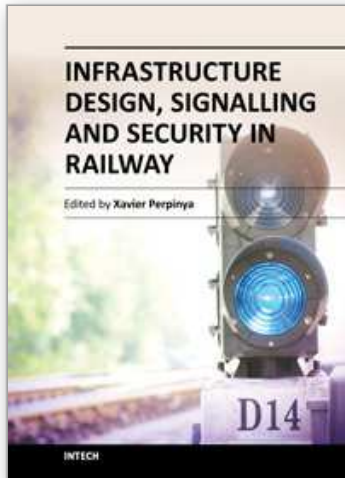
Infrastructure Design, Signalling and Security in Railway

Edited by Dr. Xavier Perpinya

Railway transportation has become one of the main technological advances of our society. Since the first railway used to carry coal from a mine in Shropshire (England, 1600), a lot of efforts have been made to improve this transportation concept. One of its milestones was the invention and development of the steam locomotive, but commercial rail travels became practical two hundred years later. From these first attempts, railway infrastructures, signalling and security have evolved and become more complex than those performed in its earlier stages. This book will provide readers a comprehensive technical guide, covering these topics and presenting a brief overview of selected railway systems in the world. The objective of the book is to serve as a valuable reference for students, educators, scientists, faculty members, researchers, and engineers.

How to reference

In order to correctly reference this scholarly work, feel free to copy and paste the following:

Mario A. Ríos and Gustavo Ramos (2012). Power System Modelling for Urban Massive Transportation Systems, Infrastructure Design, Signalling and Security in Railway, Dr. Xavier Perpinya (Ed.), ISBN: 978-953-51-0448-3, InTech, Available from: http://www.intechopen.com/books/infrastructure-design-signalling-and-security-in-railway/power-system-modelling-for-urban-massive-transportation-systems

INTECH
open science | open minds